Journal of Inorganic and General Chemistry

ZAAC

Zeitschrift für anorganische und allgemeine Chemie

Accepted Article

Title: The Temperature Effect on the Structural Features of Bidentate Ligand-Decorated Cyanide-Bridged Mn(II)-Mo(V) Compounds

Authors: Aihua Yuan

To be cited as: *Z. anorg. allg. Chem.* 10.1002/zaac.201700366

Link to VoR: http://dx.doi.org/10.1002/zaac.201700366

WILEY-VCH

www.zaac.wiley-vch.de

ARTICLE

DOI: 10.1002/zaac.2017

The Temperature Effect on the Structural Features of Bidentate Ligand-Decorated Cyanide-Bridged Mn(II)-Mo(V) Compounds

Hu Zhou,[a] Qi Chen,[b] Hui Yu,[b] Xiu-Fen Yan,[b] Ai-Hua Yuan,*[b] and Xiao-Ping Shen[c]

Keywords: Octacyanometalates; Manganese; Structure, Temperature

Abstract. The diffusion reaction of Mn^{2+} ions, the bidentate ligand dabco and $[Mo(CN)_8]^{3-}$ units at different temperatures produced 2D layer $[Mn^{II}(dabco)Mo^{V}(CN)_8]_2\cdot[Mn^{II}(H_2O)_6]\cdot 2H_2O$ (**1**) and 3D network $[Mn^{II}(dabco)]_2[Mn^{II}(CH_3OH)_4][Mo^{V}(CN)_8]_2\cdot 2H_2O$ (**2**). Structural analysis revealed that there were two independent Mn centers (Mn1 and Mn2) in the structure for each compound, which exhibited trigonal bipyramid and octahedral geometry, respectively. Notably, the coordination mode of the Mn2 unit between layers in both compounds was responsible for the resulting structural dimensionalities. The crystal growth process of final products was dominantly controlled by the kinetics. The isolation of both compounds provides an insight into the effect of crystallization temperatures on the formation and structural conversion of manganese octacyanometalates.

* Prof. A. H. Yuan
E-Mail: aihua.yuan@juest.edu.cn
[a] School of Material Science and Engineering
Jiangsu University of Science and Technology
Zhenjiang 212003, P. R. China
[b] School of Environmental and Chemical Engineering
Jiangsu University of Science and Technology
Zhenjiang 212003, P. R. China
[c] School of Chemistry and Chemical Engineering
Jiangsu University
Zhenjiang 212013, P. R. China
Supporting information for this article is available on the WWW under http://dx.doi.org/10.1002/zaac.201700xxx or from the author.

Introduction

Cyanide-bridged molecule-based magnetic materials has received intense attention in the past decades, and octacyanometalates $[M(CN)_8]^{3-}$ (M = Mo, W) are flexible building blocks which can adopt variable coordination configurations (e.g., square-antiprism, dodecahedron, bicapped trigonal-prism) depending on the surrounding geometry.[1] The assembly of $[M(CN)_8]^{3-}$ ions and the second metal centers has generated a great deal of diversified topological structures ranging from discrete entities to three-dimensional (3D) extended networks, and the resulting materials exhibited interesting magnetisms such as high T_c,[2-4] single-molecule/chain magnets,[5,6] as well as spin crossover,[7,8] etc. However, how to rationally control desired topologies with potential applications is still a great challenge.

It is well known that the design and construction of crystalline materials are closely related to the experimental conditions such as the reaction time and temperature, solvent, reagent ratio, and pH value. Especially, the synthesis temperature plays a crucial effect on adjusting the topologies and dimensionalities, because the thermal energy is proportionally dependent on the temperature. As far as we know, the temperature-driven crystal transformation phenomena were relatively rare in the $[M(CN)_8]$-based bimetallic system, although the humidity-, guest-, photo-, thermal-, pressure-, lanthanide-ion- and diffusion-reaction-induced phase conversions have been documented previously.[9-16] In this regard, the effect of crystallization temperatures on the $[M(CN)_8]$-based lanthanide-metal system have been reported recently by our group.[17-19] Studies showed that the reaction of lanthanide ions, the bidentate pillar ligand pyrazine and $[W(CN)_8]^{3-}$ units at higher temperatures (38~40 °C) gave rise to 3D pillared frameworks, while 2D layers and discrete molecules were generated upon cooling temperatures to T < 33 °C and 0 °C, respectively. That is to say, the overall structural dimensionalities for such cyanide-based bimetallic system decreased gradually upon lowing the reaction temperatures. In our ongoing research devoted to exploring the factors affecting the structures of cyanide-bridged system, the 1,4-diazabicyclo[2.2.2]octane (dabco) ligand was chosen here because of its bidentated pillar feature and a larger steric hindrance relative to pyzaine. In the present contribution, the reaction of Mn^{2+} ions, dabco and $[Mo(CN)_8]^{3-}$ at 0 °C and 25 °C isolated 2D layer $[Mn^{II}(dabco)Mo^{V}(CN)_8]_2\cdot[Mn^{II}(H_2O)_6]\cdot 2H_2O$ (**1**) and 3D network $[Mn^{II}(dabco)]_2[Mn^{II}(CH_3OH)_4][Mo^{V}(CN)_8]_2\cdot 2H_2O$ (**2**), respectively. The crystal structures and growth process of both compounds were described in detail.

Results and Discussion

Single-crystal X-ray diffraction results revealed that compound **1** forms a 2D waved layer, crystallizing in a orthorhombic space group *Pmmn*. The asymmetric unit contains two $[Mn(dabco)Mo(CN)_8]^-$ cations, one $[Mn(H_2O)_6]^{2+}$ anion and two water molecules (Fig. 1a). $[Mo(CN)_8]^{3-}$ shows a distorted square-antiprism configuration, typical for octacyanomolybdates.[20-23] Four CN species bridged to Mn1 centers and the four remaining are terminal. The average bond lengths of Mo-C and C≡N are 2.166 and 1.145 Å, respectively, and all Mo-CN linkages exhibit almost linear (175.4°-179.1°). There are two independent Mn centers (Mn1 and Mn2) in the structure. The Mn1 atoms is located in the center of a rare five-coordinated trigonal bipyramid with four cyanide-nitrogen

10.1002/zaac.201700366

and one nitrogen atom from dabco. N1, N5^{i} (symmetric code: (i) 0.5 + *x*, 1 − *y*, −*z*) and N5^{ii} (symmetric code: (ii) −*x*, 1 − *y*, −*z*) form the basic plane with Mn-N distances of 2.129-2.148 Å, while N4^{iii} (symmetric code: (iii) *x*, *y*, z − 1) and N6 occupy two apical positions with slightly longer Mn-N lengths of 2.173 to 2.386 Å. All Mn1-NC units are bent significantly with angles of 164.9-172.8°, in contrast to the linear Mo-CN bonds. In the $[Mn(H_2O)_6]^{2+}$ unit, Mn2 shows a slightly distorted octahedral geometry. The equatorial plane and apical sites are all occupied by water molecules with Mn-O distances of 2.100-2.391 Å. The coordinated geometry and parameters of Mn2 were relatively common in the $M^{V/IV}(CN)_8$-Mn^{II} compounds.[24,25] Then, Mo1 and Mn1 centers are linked alternatively by CN groups, generating a 2D waved grid-like layer (Fig. 1b, Fig. 1c), as found in $(tetrenH_2)_{0.5}[Mn^{II}(H_2O)_2][Mo^{V}(CN)_8]\cdot 2H_2O$[26] and $\{(tetrenH_5)_{0.8}Cu^{II}_4[W^{V}(CN)_8]_4\cdot 7.2H2O\}_n$.[27] In each four-metallic 12-atom grid, Mo1 and Mn1 atoms lie on the vertexes and cyanide bridges form the sides. The diagonal distances for each grid are about 9.022 Å (Mo1···Mo1) and 5.929 Å (Mn1···Mn1). Furthermore, four terminal cyanide-nitrogen atoms in $[Mo(CN)_8]^{3-}$ interact with oxygen atoms of $[Mn(H_2O)_6]^{2+}$ through O-H···N hydrogen bonds. As shown in Fig. 1d, the neighboring $[Mn(dabco)Mo(CN)_8]^{-}$ anionic layers are well separated by $[Mn(H_2O)_6]^{2+}$ cationic moieties through the weak hydrogen bonds, isolating a 3D supramolecular structure (Fig. 1d). Interestingly, these $[Mn(H_2O)_6]^{2+}$ moieties between layers are interconnected by oxygen bridges along the *a* axis, generating a 1D linear chain (Fig. 1e).

Table 1. Crystallographic data and structural refinement for compounds **1** and **2**.

Compound	**1**	**2**
Formula	$Mn_3Mo_2C_{28}H_{40}N_{20}O_8$	$Mn_3Mo_2C_{32}H_{44}N_{20}O_6$
M_r	1141.50	1161.57
Crystal system	orthorhombic	triclinic
Space group	*Pmmn*	*P*-1
a /Å	9.4953(19)	8.2727(18)
b /Å	35.000(7)	9.5980(12)
c /Å	8.1770(17)	14.3150(13)
a /°	90.00°	87.286(3)
b /°	90.00°	87.223(2)
g/°	90.00°	86.064(3)
V /Å^3	2717.5(10)	1131.5(3)
Z	2	1
ρ_c /g cm^{-3}	1.395	1.705
μ /mm^{-1}	1.182	1.418
Total, unique	22345, 3189	8834, 4350
Observed [$I > 2\sigma(I)$]	1906	3503
GOF on F^2	1.062	1.037
R_1, wR_2 [$I > 2\sigma(I)$]	0.0571, 0.1407	0.0513, 0.1267
R_1, wR_2 (all data)	0.0743, 0.1427	0.0561, 0.1280

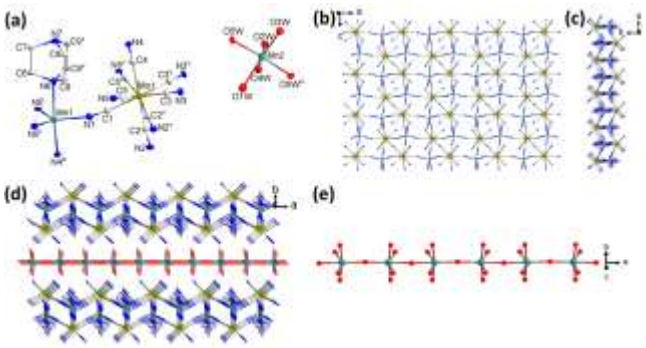

Figure 1. (a) Molecular drawing of compound **1**. All H atoms and uncoordinated water molecules are omitted for clarity. Symmetry codes: (i) *x* + 1/2, −*y* + 1, −*z*; (ii) −*x*, −*y* + 1, −*z*; (iii) *x*, *y*, *z* − 1; (v) −*x* + 1/2, *y*, *z*. (b) the 2D layer in the *ac* plane (dabco ligands were omitted for clarity.); (c, d) the 2D layer in the *ab* plane; (e) the 1D $[Mn(H_2O)_6]^{2+}$ cationic chain along the *a* axis.

Compound **2** has a 3D structure, which crystallized in a triclinic space group *P*-1. The asymmetrical unit composes of one $\{[Mn(dabco)]_2[Mn(CH_3OH)_4]\}^{6+}$ moiety, two $[Mo(CN)_8]^{3-}$ units as well as guest water molecules (Fig. 2a). Similar to compound **1**, the Mo1 and Mn1 atoms in compound **2** display a square antiprism and trigonal bipyramid, respectively. However, the obvious difference in the structures between both compounds is the coordination geometry of Mn2. All Mn2 atoms in compound **2** have an octahedral configuration, where the equatorial plane is filled by methanol molecules, and the apical sites are occupied by cyanide groups. The average bond distance of Mn2-O is 2.200 Å, comparable to 2.249 Å of the Mn2-N bond, respectively. The $[Mo(CN)_8]^{3-}$ unit provides five bridged cyanides coordinating to Mn(II) ions, of which four coordinate to Mn1 to form a waved layer (Fig. 2b, Fig. 2c) and one to Mn2 further connecting these layers to generate a 3D network (Fig. 2d), as observed in $(NH_4)_2[Mn^{II}(CH_3OH)_4][Mn^{II}(DMF)]_2[Mo^{IV}(CN)_8]_2$.[28] To some extent, these $[Mn(CH_3OH)_4]^{2+}$ units can be regarded as pillars linking adjacent layers (Fig. 2e), which are similar to the construction mode of the Hofmann-type system.[29-31]

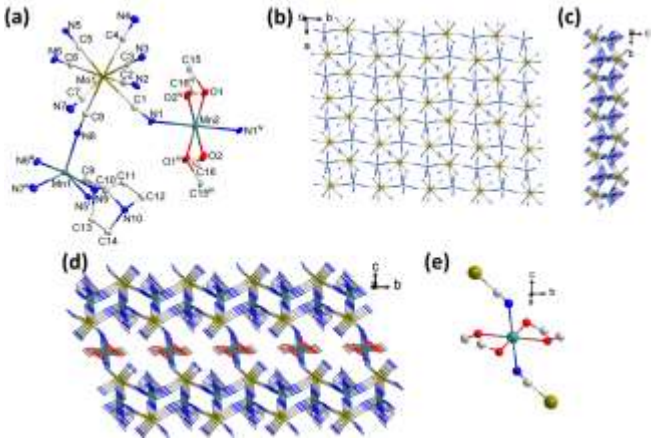

Figure 2. (a) Molecular drawing of compound **2**. All H atoms and uncoordinated water molecules are omitted for clarity. Symmetry codes: (i) *x*, *y* + 1, *z*; (ii) −*x* + 1, −*y*, −*z* + 2; (iii) −*x* + 2, −*y*, −*z* + 2; (iv) −*x* + 1, −*y*, −*z* + 1. (b) the 2D layer in the *ab* plane (dabco ligands were omitted for clarity.); (c, d) the 2D layer in the *bc* plane; (e) the $[Mn(CH_3OH)_4]^{2+}$ unit.

10.1002/zaac.201700366

Except for the structural descriptions of both compounds, the factors affecting the architectures of final products were also investigated. Studies revealed that the crystals of compound **1** were only isolated at lower temperatures (T < 10 °C) and any phase transformation didn't happen upon prolonging the diffusion time. In contrast, compound **2** was obtained at higher temperatures (T > 25 °C). In fact, the formation of both compounds at different temperatures can be reasonably explained from the view of kinetic as follows. In our case, the bonding of unsaturated-coordinately sites of octahedral Mn atoms to solvent molecules needs a lower activation barrier at low temperatures. In addition, prolonging the reaction time was not enough to overcome the activation barrier losing part of coordinated solvent molecules, and then the 2D compound **1** was formed. For compound **2**, however, the coordination of octahedral Mn moieties between adjacent layers to Mo atoms in the layer through cyanide groups needs to overcome a significant activation barrier. Hence, these crystals of 3D compound **2** were only isolated at higher temperatures. In other words, the activation energy barrier increased with decreasing the number of coordinated solvents involved in the structure. On the basis of above analysis, we can conclude that the temperature of diffusion reaction is a determining factor on the final structures. The crystal growth process for such system was controlled dominantly by the kinetics, and compound **2** was the most kinetically favored product. Notably, the crystals of compound **1** have not been observed with the naked eye during the whole growing process of compound **2**, which can be reasonably attributed to the fast crystallization rate of compound **2**. As a result, there's no enough time for the nucleation and crystal growth of compound **1**, leading to the one-step crystallization of compound **2**.

Variable-temperature magnetic susceptibility for compound **2** was measured on the polycrystalline samples in an applied field of 2 kOe (Figure 3). The $\chi_M T$ values (per $Mn^{II}_3Mo^{V}_2$) at 300 K is 13.46 cm^3 K mol^{-1}, which is consistent with the spin-only value of 13.79 cm^3 K mol^{-1} calculated for the $Mn^{II}_3Mo^{V}_2$ unit (S_{Mo} = 1/2, S_{Mn} = 5/2) assuming g_{Mo} = g_{Mn} = 2.0. The $\chi_M T$ value keeps almost constant upon cooling to about 30 K, and then abruptly decreases to 7.08 cm^3 K mol^{-1} at 1.8 K. Such behavior is an indication of the antiferromagnetic interaction between Mo^V and Mn^{II} ions. The Curie-Weiss fitting gives the Weiss constant of -50 K, indicative of the antiferromagnetic $Mo^V\cdots Mn^{II}$ interaction involved in such compound.

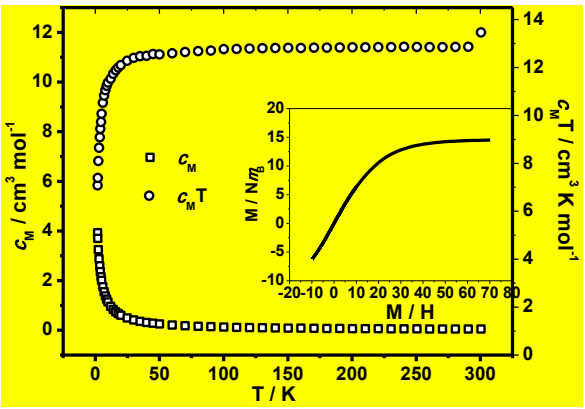

Figure 3. The variable-temperature magnetic susceptibilities for compound **2** (Inset: Field dependence of the magnetization.).

Variable-field magnetization at 1.8 K for compound **2** showed that the magnetization moderately increases and reaches to the saturation value of 14.52 $N\varepsilon_B$ at 70 kOe (Figure 3 inset). The saturation value is slightly higher than the theoretical one (13 $N\varepsilon_B$, calculated from $M_S = g(3S_{Mn} - 2S_{Mo})$ with g = 2.0) for antiferromagnetic coupled $Mn^{II}_3Mo^{V}_2$ unit, further confirming the antiferromagnetic nature. No obvious hysteresis loop was observed (Fig. S2), precluding the ferrimagnetic property.

Conclusions

In summary, two bidentate ligand-decorated Mn(II)-Mo(V) compounds with different structural dimensionalities were obtained by varying diffusion-reaction temperatures. Viewed from a molecular level, the coordination configuration of Mn2 between layers has played a key role on the self-assembly process. Especially, the kinetics favored products can be generated at higher temperatures. The successful construction of both compounds not only produced interesting examples of cyanide-bridged molecular materials, but also provided valuable information on the inherit relations between temperatures and architectures. Further work will focus on the temperature-driven structural conversion of octacyanide-bridged compounds with other transition-metal ions or bidentate pillar ligands.

Experimental Section

Materials and General Methods: Unless otherwise mentioned, all reactants were used as purchased without further purification. All chemicals and solvents were purchase from commercial sources and used as received. The $[HN(n\text{-}C_4H_9)_3]_3Mo(CN)_8$ precursor was prepared according to the published procedure.[32] The elemental analyses were performed on a PerkinElmer 240C elemental analyzer. Infrared (IR) spectra were recorded over the range 4000-400 cm^{-1} using a Nicolet FT 1703X spectrometer (KBr pellets). Powder X-ray diffraction data were collected on a Shimadzu XRD-6000 diffractometer with Cu-K_a radiation.

Syntheses. At 0 °C, a small glass vial (3 mL) containing $MnCl_2\cdot 4H_2O$ (0.05 mmol) and 1,4-diazabicyclo[2.2.2]octane (dabco) (0.10 mmol) was placed carefully into a big glass vial (15 mL) containing $[HN(n\text{-}C_4H_9)_3]_3[Mo(CN)_8]\cdot 4H_2O$ (0.05 mmol). Both vials were filled slowly with a water-methanol (V/V = 1/1) solvent until the solution in the big vial was over the small vial 1 cm, and then the big vial was sealed. After allowing both vials to stand in dark for one week, pale-yellow plate-like crystals of $[Mn(dabco)Mo(CN)_8]_2\cdot[Mn(H_2O)_6]\cdot 2H_2O$ (**1**) were formed in the small vial. Unfortunately, the crystals of **1** were easily fragile once exposed to the air, together with the structural collapse which was confirmed by X-ray diffraction patterns (Fig. S1a). Interestingly, yellow plate-like crystals of $[Mn(dabco)]_2[Mn(CH_3OH)_4][Mo(CN)_8]_2\cdot 2H_2O$ (**2**) were obtained when changing the temperature of solution to 25 °C. In contrast, the crystals of compound **2** were stable in the air (Fig. 1b). Anal. Calcd (%) for $C_{32}H_{44}Mn_3N_{20}O_6Mo_2$ (**2**): C: 33.09; H, 3.82; N, 24.12. Found: C, 33.23; H, 3.70; N, 24.27. IR (KBr) for compound **2**: 2141 and 2122 cm^{-1} for ν (C≡N).

X-ray Crystallographic Analysis: Single crystal X-ray diffraction data were collected with a Bruker Apex II diffractometer with Mo-K_α radiation at 173 K. For compound **1**, the X-ray structural measurement was carried out by covering liquid paraffin on a

single crystal. The structures were solved by Patterson methods and refined by a full-matrix least-squares technique with the *SHELXTL* program package.[33] All non-H atoms were refined anisotropically. The positions of H atoms from dabco and methanol were calculated geometrically, while the H atoms of water molecules were found from differential Fourier maps and refined isotropically with U_{iso} = 1.2 U_{iso}(O). The lattice water molecules (O6W, O7W) in compound **1** are disordered with an occupancy of 25%, which caused the short inter D...A contact between these water molecules. The details of crystal data collections and structural refinement parameters are summarized in Table 1. Selected bond distances and angles are listed in Table S1 and Table S2.

Supporting Information (see footnote on the first page of this article): Powder XRD patterns of compounds **1** and **2**. Selected bond lengths and angles of compounds **1** and **2**; CCDC numbers: 1572385(**1**) and 1572386(**2**). This data can be obtained free of charge from the Cambridge Crystallographic Data Centre via www.ccdc.cam.ac.uk/data_request/cif.

Acknowledgements

This work was supported by the National Natural Science Foundation (51672114, 51272095, 51402131), Natural Science Foundation of Jiangsu Province (BK20151328, BK20161357, BK20140514), and the project of the Priority Academic Program Development of Jiangsu Higher Education Institutions.

References

[1] B. Sieklucka, R. Podgajny, T. Korzeniak, B. Nowicka, D. Pinkowicz, M. Kozieł, *Eur. J. Inorg. Chem*. **2011**, 305−326.

[2] T. W. Wang, J. Wang, S. Ohkoshi, Y. Song, X. Z. You, *Inorg. Chem*. **2010**, *49*, 7756−7763.

[3] W. Kosaka, K. Imoto, Y. Tsunobuchi, S. Ohkoshi, *Inorg. Chem*. **2009**, *48*, 4604−4606.

[4] D. Pinkowicz, R. Podgajny, M. Bałanda, M. Makarewicz, B. Gaweł, W. Łasocha, B. Sieklucka, *Inorg. Chem*. **2008**, *47*, 9745−9747.

[5] T. S. Venkatakrishnan, S. Sahoo, N. Bréfuel, C. Duhayon, C. Paulsen, A. Barra, S. Ramasesha, J. P. Sutter, *J. Am. Chem. Soc*. **2010**, *132*, 6047−6056.

[6] J. H. Lim, J. H. Yoon, H. C. Kim, C. S. Hong, *Angew. Chem., Int. Ed*. **2006**, *45*, 7424−7426.

[7] S. Ohkoshi, K. Imoto, Y. Tsunobuchi, S. Takano, H. Tokoro, *Nat. Chem*. **2011**, *3*, 564−569.

[8] M. Arai, W. Kosaka, T. Matsuda, S. Ohkoshi, *Angew. Chem., Int. Ed*. **2008**, *47*, 6885−6887.

[9] H. Zhou, Q. Chen, H. B. Zhou, X. Z. Yang, Y. Song, A. H. Yuan, *Cryst. Growth Des*. **2016**, *16*, 1708−1716.

[10] N. Ozaki, H. Tokoro, Y. Miyamoto, S. Ohkoshi, *New. J. Chem*. **2014**, *38*, 1950−1954.

[11] N. Ozaki, H. Tokoro, Y. Hamada, A. Namai, T. Matsuda, S. Kaneko, S. Ohkoshi, *Adv. Funct. Mater*. **2012**, *22*, 2089−2093.

[12] D. Pinkowicz, K. Kurpiewska, K. Lewiński, M. Balanda, M. Mihalik, M. Zentová, B. Sieklucka, *CrystEngComm* **2012**, *14*, 5224−5229.

[13] R. Podgajny, S. Chorąży, W. Nitek, A. Budziak, M. Rams, C. J. Gómez-García, M. Oszajca, W. Łasocha, B. Sieklucka, *Cryst. Growth Des*. **2011**, *11*, 3866−3876.

[14] B. Nowicka, M. Bałanda, B. Gaweł, G. Ćwiak, A. Budziak, W. Łasocha, B. Sieklucka, *Dalton Trans*. **2011**, *40*, 3067−3073.

[15] R. Gheorghe, M. Kalisz, R. Clérac, C. Mathonière, P. Herson, Y. L. Li, M. Seuleiman, R. Lescouëzec, F. Lloret, M. Julve, *Inorg. Chem*. **2010**, *49*, 11045−11056.

[16] A. H. Yuan, P. D. Southon, D. J. Price, C. J. Kepert, H. Zhou, W. Y. Liu, *Eur. J. Inorg. Chem*. **2010**, 3610−3614.

[17] H. Zhou, G. W. Diao, X. Z. Yang, A. H. Yuan, M. Zhang, J. Sun, *Z. Anorg. Allg. Chem*. **2013**, *639*, 2276−2281.

[18] H. Zhou, G. W. Diao, S. Y. Qian, X. Z. Yang, A. H. Yuan, Y. Song, Y. Z. Li, *Dalton Trans*. **2012**, *41*, 10690−10697.

[19] H. Zhou, A. H. Yuan, S. Y. Qian, Y. Song, G. W. Diao, *Inorg. Chem*. **2010**, *49*, 5971−5976.

[20] S. L. Ma, Y. Ma, S. Ren, S. P. Yan, P. Cheng, Q. L. Wang, D. Z. Liao, *Cryst. Growth Des*. **2008**, *8*, 3761−3765.

[21] J. H. Lim, Y. S. You, H. S. Yoo, J. H. Yoon, J. II. Kim, E. K. Koh, C. S. Hong, *Inorg. Chem*. **2007**, *46*, 10578-10586.

[22] Y. S. You, J. H. Yoon, J. H. Lim, H. C. Kim, C. S. Hong, *Inorg. Chem*. **2005**, *44*, 7063−7069.

[23] Y. S. You, D. Kim, Y. Do, S. J. Oh, C. S. Hong, *Inorg. Chem*. **2004**, *43*, 6899−6901.

[24] F. L. Yang, A. H. Yuan, H. Zhou, H. B. Zhou, D. Yang, Y. Song, Y. Z. Li, *Cryst. Growth Des*. **2015**, *15*, 176−184.

[25] A. H. Yuan, H. Zhou, G. W. Diao, P. D. Southon, C. J. Kepert, L. Liu, *Int. J. Hydrogen Energ*. **2014**, *39*, 884−889.

[26] S. L. Ma, S. Ren, D. Z. Liao, S. P. Yan, *Struct. Chem*. **2009**, *20*, 145−154.

[27] R. Podgajny, T. Korzeniak, M. Balanda, T. Wasiutynski, W. Errington, T. J. Kemp, N. W. Alcock, B. Sieklucka, *Chem. Commun*. **2002**, 1138−1138.

[28] Y. Guo, X. F. Tang, Y. Song, X. M. Ren, *Inorg. Chem. Commun*. **2014**, *45*, 79−81.

[29] J. T. Culp, C. Madden, K. Kauffman, F. Shi, C. Matranga, *Inorg. Chem*. **2013**, *52*, 4205−4216.

[30] N. Sciortino, K. R. Scherl-Gruenwald, G. Chastanet, G. J. Halder, K. W. Chapman, J. F. Létard, C. J. Kepert, *Angew. Chem., Int. Ed*. **2012**, *51*, 10154−10158.

[31] X. Chen, H. Zhou, Y. Y. Chen, A. H. Yuan, *CrystEngComm* **2011**, *13*, 5666−5669.

[32] L. D. C. Bok, J. G. Leipoldt, S. S. Basson, *Z. Anorg. Allg. Chem*. **1975**, *415*, 81−83.

[33] G. M. Sheldrick, *SHELXTL-97. Program for crystal structure refinement*, University of Göttingen, Germany, **1997**.

Received:
Published online:

10.1002/zaac.201700366

Entry for the Table of Contents

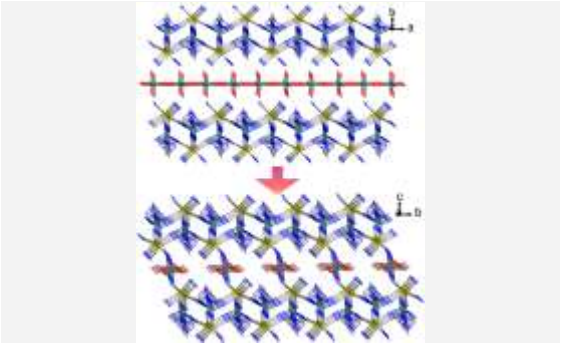

Hu Zhou, Qi Chen, Hui Yu, Xiu-Fen Yan, Ai-Hua Yuan,* and Xiao-Ping Shen

The Temperature Effect on the Structural Features of Bidentate Ligand-Decorated Cyanide-Bridged Mn(II)-Mo(V) Compounds